Study on Frost Heave Control Measures and Their Effectiveness for Existing Railway Subgrades in Cold Regions

Yugang Ren[1*], Honglin Ding[2], Liwen Zhang[2], Yin Chen[1]

[1]Lanzhou Jiaotong University, Lanzhou, China
[2]China Railway Lanzhou Group Co., Ltd., Lanzhou, China

*Corresponding author's email: renyugang123@qq.com

Abstract. In order to mitigate the impacts of disasters such as frost heave, thawing, and settlement on railway subgrades in cold regions, and based on the theory of frozen soil frost heave while considering the influence of solar radiation, this paper proposes an insulation and waterproofing measure to prevent frost heave in these subgrades. A transient numerical model for the water-heat-force coupling of frost heave in subgrades is established, and its feasibility is validated by comparing on-site measured data with simulation results. The effectiveness of the proposed insulation and waterproofing measures is further validated by comparing the frost heave mitigation effects between the original and treated subgrades.Research shows that the uneven frost heave of the subgrade is aggravated by the sunny-shady slope effect caused by solar radiation. The primary cause of frost heave is the accumulation of moisture in the fine-grained clay layer of the subgrade.Compared to the original subgrade, the treated subgrade exhibits a more uniform temperature distribution and a smaller temperature gradient, significantly mitigating the sunny-shady slope effect. This helps alleviate uneven frost heave, as well as surface melting and subsidence. Additionally, it reduces the annual variation in displacement, minimizes vertical frost heave displacement, and enhances the stability of the subgrade structure, effectively managing frost heave issues in existing railway subgrades.

Keywords: Railway subgrade; Heat preservation; Waterproof; Anti-frostbite swelling; Numerical simulation

1 Introduction

The term frozen soil refers to soil or rock that remains below 0°C and contains ice. Permafrost is widely distributed in China, making it the third-largest frozen soil region in the world [1]. In recent years, with the rapid development of transportation infrastructure in China, large-scale construction of railway transportation facilities in frozen soil areas has been carried out. However, due to the unique characteristics of frozen soil, disasters such as frost heaving, thaw subsidence, and embankment collapse have occurred in the existing railway subgrade in frozen soil regions under low- temperature

W. Nie et al. (eds.), *Proceedings of the 2024 6th International Conference on Hydraulic, Civil and Construction Engineering (HCCE 2024)*, Atlantis Highlights in Engineering 37,
https://doi.org/10.2991/978-94-6463-726-7_81

conditions. frozen soil-related embankment frost heaving damage has become one of the key factors restricting the safe operation of railways in China's frozen soil regions [2].

In recent years, there have been many advances in the research on frost heave diseases of frozen soil roadbeds. In the study of the mechanism and driving factors of soil frost heave. WANG et al [3] found that the cause of frozen soil is that the fine soil particle structure absorbs water and expands during the freezing process, leading to the easy occurrence of frost heave in fine soil particles. AGGESTAM E et al [4] use geosynthetic materials to achieve drainage, reinforcement, and anti-seepage, reducing the risk of roadbed settlement degradation. In terms of frost heave monitoring and numerical simulation research. PIOTROVICH A et al [5] have studied a real-time frost heave monitoring system to dynamically monitor roadbed temperature and deformation parameters. ZHAO et al [6] monitored and calculated the impact of frost heave on the surface track structure based on the characteristics of frost heave height of roadbeds in cold regions.

In summary, there is currently a lack of in-depth discussion on the insulation, waterproofing, and anti freezing measures for existing railway subgrades in permafrost regions. In response to these issues, this paper takes the frost heave-damaged section of the Lanxin Railway as the research subject and proposes insulation, waterproofing, and anti-frost heave measures for the subgrade of existing railways. A water-heat-force coupled transient frost heave calculation model for the subgrade is established. The feasibility of the numerical model is verified by comparing it with field experimental data, and the water-thermal variation process in the subgrade is analyzed. The effectiveness of the proposed insulation, waterproofing, and anti-frost heave measures is studied, aiming to provide a reference and basis for the mitigation of frost heave diseases in the subgrade of existing railways.

2 Roadbed Anti Freezing Measures

The overall cross-sectional form of the existing railway subgrade is an axisymmetric structure along the longitudinal centerline of the subgrade, with the lower part of the subgrade consisting of a silty clay frost heave layer and the upper part consisting of a subgrade filling layer. Based on the disaster mechanism of roadbed frost heave and thaw settlement, a new type of insulation, waterproof and anti freezing roadbed structure is proposed, which is specifically set as follows: ① Set waterproof geotextile on the surface of the roadbed to block the water inlet channel of the roadbed, prevent rainwater infiltration and reduce the moisture content of the roadbed; ② Set gravel cushion layer on the upper and lower sides of waterproof geotextile to protect the waterproof fabric from being crushed and punctured; ③ Using steel plastic geogrids to increase the impact resistance of the roadbed and improve the structural strength of the roadbed; ④ Injecting foam adhesive into the ballast layer not only maintains the structural strength of the ballast layer, but also provides thermal insulation for the roadbed Cover the slope, shoulder, and foot of the roadbed with polyurethane insulation board to cut off the convective heat transfer channel between the external environment and the roadbed, in order to achieve insulation, waterproofing, and anti-seepage effects. The specific settings are shown in Figure 1.

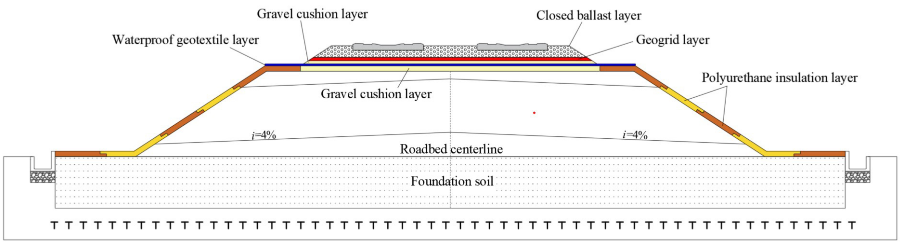

Fig. 1. Railway roadbed anti freezing and anti swelling structure

3 Three Field Coupling Model of Frozen Soil Water Heat Force

3.1 Water Heat Coupling Control Equation

The water-heat coupling process of the subgrade permafrost is accompanied by the generation of latent heat from the ice-water phase change. Using the phase change latent heat as the heat source and based on the law of energy conservation, the heat transfer equation for porous media is derived according to Fourier's law [7]:

$$\rho C \frac{\partial T}{\partial t} = \lambda \cdot \nabla^2 T + L\rho_i \frac{\partial \theta_i}{\partial t} \tag{1}$$

where ρ refers to the unit body density (kg/m^3); C refers to the equivalent volumetric heat capacity of unit body (J/(kg·K)); T refers to the temperature of soil (°C); θ_i is the volume content of ice (%); t is the time (s); λ refers to the Heat conductivity coefficient of unit body (W/(m·K)); L is the latent heat of phase change (334.5kJ/kg); ∇ is the Laplacian operator. The thermal parameters of soil are determined by the parameters of soil particles, unfrozen water, and frozen ice:

$$\begin{cases} \lambda = \lambda_s^{\theta_s} \cdot \lambda_w^{\theta_w} \cdot \lambda_i^{\theta_i} \\ \rho C = \rho_w C_w \theta_w + \rho_s C_s \theta_s + \rho_i C_i \theta_i \\ \theta_w + \theta_s + \theta_i = 1 \end{cases} \tag{2}$$

where θ_s and θ_w are the volume contents of soil particles and unfrozen water, respectively (%); C_s, C_w and C_i are the specific heat capacities of soil particles, unfrozen water, and ice, respectively (J/(kg·K)); λ_s, λ_w and λ_i refers to the thermal conductivity coefficients of soil particles, unfrozen water, and ice, respectively (W/(m·K)); ρ_s, ρ_w and ρ_i are the densities of soil, unfrozen water, and ice, respectively (kg/m^3).

For the freeze-thaw process of heterogeneous porous subgrade, the migration process of unfrozen water in the subgrade is described by the Richards equation. Assuming that the freeze-thaw process of frozen soil is similar to the water migration process of unsaturated soil, the water migration equation of unsaturated soil is derived based on the law of conservation of mass [8]:

$$\frac{\partial \theta_w}{\partial t}+\frac{\rho_i}{\rho_w}\frac{\partial \theta_i}{\partial t}=\nabla\left[D(\theta_w)\nabla\theta_w+k(\theta_w)\right] \tag{3}$$

Considering the influence of freezing and freezing in soil on water migration, an impedance factor is introduced to characterize the blocking effect on water migration. Therefore, the water diffusion rate $D(\theta_w)$ in frozen soil is calculated using the following formula:

$$D(\theta_w)=\frac{k(\theta_w)}{c(\theta_w)}\cdot 10^{-10\theta_i} \tag{4}$$

where $c(\theta_w)$ is the specific water capacity. The permeability coefficient $k(\theta_w)$ of unsaturated soil is taken according to the Gardner model [9]:

$$k(\theta_w)=k_s\cdot S^l\left[1-\left(1-S^{1/m}\right)^m\right]^2 \tag{5}$$

$$S=\frac{\theta_w-\theta_r}{\theta_s-\theta_r} \tag{6}$$

where m and l are all soil parameters; k_s is the Saturated soil permeability coefficient; S is the relative saturation of soil mass (%); θ_s refers to saturated water content; θ_r is the residual moisture content. In the process of hydrothermal coupling, the solid-liquid ratio $B(T)$ is introduced to represent the proportion of ice water volume in frozen soil, and a connection equation for hydrothermal field coupling is constructed [10]:

$$B(T)=\frac{\theta_i}{\theta_u}=\begin{cases}1.1\left(\dfrac{T}{T_f}\right)^{\alpha}-1 & T<T_f\\ 0 & T\geq T_f\end{cases} \tag{7}$$

where T_f is the soil freezing temperature (K); α is the test parameters, typical range for silty clay is 0.47-0.56.

In summary, by combining equations (1) to (7), a transient numerical calculation model for coupled freeze-thaw heave of subgrade water heat force is obtained, which describes the dynamic evolution mechanism of temperature and moisture in subgrade soil.

3.2 Custom Mathematical Model for Water Heat Coupling

Based on the water heat coupling control equation, a coefficient type partial differential equation is customized through the PDE module to establish a numerical model for the water heat coupling of frozen soil subgrade. The generalized expression of the coefficient type partial differential equation is as follows:

$$e_a \frac{\partial^2 S}{\partial t^2} + d_a \frac{\partial S}{\partial t} + \nabla \cdot \left(-c\nabla S - \alpha S + \gamma\right) + \beta \cdot \nabla S + aS = f \tag{8}$$

where S is the dependent variable field matrix; e_a is the quality coefficient; d_a is the damping coefficient; c is the diffusion coefficient; α is the conservation flux convection coefficient; γ is the conservation flux source; β is the convection coefficient; a is the absorption coefficient; f is the source item.

Substitute equation (7) into equation (1) to obtain the custom interface equation for the temperature field of the coefficient type partial differential equation:

$$\rho C(\theta)\frac{\partial T}{\partial t} + \nabla \cdot \left(-\lambda(\theta)\nabla T\right) = L \cdot \rho_i \cdot (\theta_s - \theta_r) \cdot \left[\frac{\partial B(T)}{\partial T}\frac{\partial T}{\partial t} \cdot S + B(T) \cdot \frac{\partial S}{\partial t}\right] \tag{9}$$

Substitute equation (7) into equation (3) and use the relative saturation of frozen soil instead of the amount of soil icing to obtain the custom interface equation for the coefficient type partial differential equation of the water distribution field:

$$\left(1 + \frac{\rho_i}{\rho_w} B(T)\right)\frac{\partial S}{\partial t} + \frac{\rho_i}{\rho_w} \cdot \frac{\partial B(T)}{\partial t} \cdot S = \nabla\left[D(S)\nabla S + k(S)\right] \tag{10}$$

4 Simulation Calculation of Railway Subgrade Frost Heave

In order to conduct in-depth research on the disaster mechanism of railway subgrade frost heave in frozen soil areas, the frost heave disease section of Lanxin Railway subgrade is taken as the research object. Considering the influence of solar radiation and convective heat transfer of the medium, a transient mathematical model of water heat force coupling for subgrade frost heave is established to calculate the changes in moisture, temperature and displacement of the new subgrade and the original subgrade. The treatment effect of the new railway subgrade insulation and waterproof anti frost heave structure is compared and analyzed, and the feasibility and effectiveness of the anti frost heave structure are verified.

4.1 Engineering Geological Conditions

The on-site test site is located in the K411 section of the Jinchang Shandan section of the Jiling area of the Lanxin Railway in Gansu Province. It is situated in the central part of the Hexi Corridor, adjacent to the Qilian Mountains to the south, with an altitude of approximately 2120 m. The topography of the Longshou Mountain front structural basin where this section of the line is located is in the form of a alluvial gravel Gobi plain, with an aquifer consisting of alluvial mudstone gravel and sandy clay layers, and a soil layer under the roadbed consisting of silty clay and weakly weathered mudstone interbedded with sandstone layers. The main source of supply for diving comes from the infiltration of rainwater and floodwater discharged from the valley, as well as the snowmelt groundwater in the bedrock fissures of Longshou Mountain. The average temperature in the Jiling area from November to February of the following year is -5 °C to -20 °C, with an extreme minimum temperature of around -35 °C. According to on-site roadbed monitoring data, the maximum freezing depth is about 1.43 m and the maximum frost heave height is 45 mm.

4.2 Geometric Model

Based on the geological survey data of Lanxin Railway, establish a two-dimensional model of the roadbed as shown in Figure 2. The height of the roadbed filling layer is 3.5 m, the width of the road surface is 13.4 m, and the slope gradient is 1:1.5. The part extending horizontally outward from the foot of the slope on both sides of the roadbed is the natural surface, and the lower part of the roadbed is a 5 m thick layer of silty clay and an 8 m thick layer of weathered rock. The hydrothermal parameters of roadbed materials are summarized in Table 1.

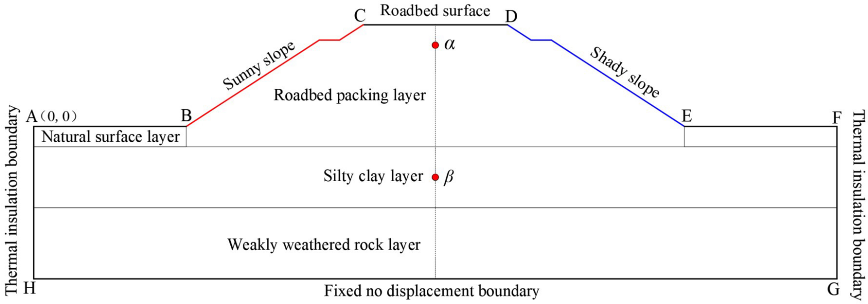

Fig. 2. Schematic diagram of two-dimensional model of railway subgrade

Table 1. Thermal parameters of subgrade materials

Material	ρ/ (kg·m^{-3})	C/ (kJ·kg^{-1}·K^{-1})	λ/ (W·m^{-1}·K^{-1})	k_u/ (m·pa^{-1}·s^{-1})	θ_s	θ_r
Filler	2245	782	1.410	1E-4	0.40	0.05
Surface soil	1630	943	1.680	15E-2	0.38	0.05
Silty clay	1800	1120	1.125	1E-7	0.41	0.06
Granite	2800	800	2.830	75E-2	0.07	0.01

4.3 Physical Field Parameters and Boundary Conditions

For the temperature boundary conditions of the model, the AH and FG boundaries are set as thermal insulation boundaries, the heat source flux of the HG boundary is 0.08 w/m^2, the maximum temperature of the external environment is 20 °C, and the minimum temperature is -10 °C. Periodic temperature boundary conditions shall be set for the surface of the roadbed, shaded slope, sunny slope, and roadbed surface [11]. The model runs for 365 days.

The frost heave deformation of the roadbed in frozen soil areas is mainly concentrated on the surface of the roadbed. The HG boundary at the bottom of the model is set as a fixed non displacement boundary, and considering the lateral constraints around the foundation, the displacement of the HABDFG boundary in the x direction is set to 0 and the y direction is set as a free displacement boundary. According to local meteorological data and on-site measurements, the total annual precipitation in the Jinchang Shandan section of the Lanxin Railway is ≤ 261 mm, and the precipitation is mainly concentrated from June to October. The soil moisture content of the roadbed within the freezing depth of K411 section, which is severely frozen on the Lanxin Railway, is between 18% and 30%, without considering the replenishment effect of rainfall and groundwater. The initial values of the roadbed moisture field are set according to the moisture content of different layers of materials, and the moisture content of the roadbed surface and filling layer, natural soil surface layer, silty clay layer, and weathered rock layer are taken as 12%, 15%, 25%, and 10%, respectively.

5 Result and Analysis

5.1 Comparative Analysis of Roadbed Temperature Field

After one cycle (1a), the temperature change of the roadbed tends to stabilize, and the temperature distribution of the original roadbed and the treated roadbed is extracted. As shown in Figures 3a and 3b, except for the sunny-shady slopes and the surface boundary layer, the temperature inside the roadbed is approximately symmetrically distributed along the centerline of the roadbed. This is because the influence of winter solar radiation on the temperature of the soil inside the roadbed is relatively small, while the heat absorption effect on the surface of the roadbed is more obvious, resulting in the surface temperature of the roadbed being higher than the temperature of the soil on both sides of the slope. Secondly, regarding the temperature distribution of the treated roadbed, the polyurethane insulation board covering the outside of the roadbed blocks the heat exchange channel between the roadbed soil and the external environment, resulting in less convective heat transfer between the soil and the environment. The overall temperature distribution of the roadbed is uniform, with a small temperature gradient, and is not affected by solar radiation, forming a sunny-shady slopes effect. Under the same working conditions, the highest temperature of the original roadbed is 3.62 °C and the lowest temperature is -8.37 °C; The maximum temperature of the treated roadbed is 4.47 °C and the minimum temperature is -7.24 °C. The maximum freezing depth of the original roadbed soil is located about 2.8 m below the natural surface, while the maximum freezing depth of the treated roadbed is located about 1.1m below the natural surface.

Extract the temperature at the domain point probes α and β of the original and treated roadbeds, as shown in Figures 4a and 4b. The temperature at different positions of the treated roadbeds is higher than that of the original roadbeds, and the temperature variation of the treated roadbeds is relatively small within the year. From this, it can be seen that the annual temperature variation of the roadbed treated with anti freezing measures is relatively small, and the insulation effect is good, reducing the sunny-shady slopes effect caused by solar radiation, which is conducive to reducing the uneven frost heave degree of the roadbed and enhancing its anti freezing ability.

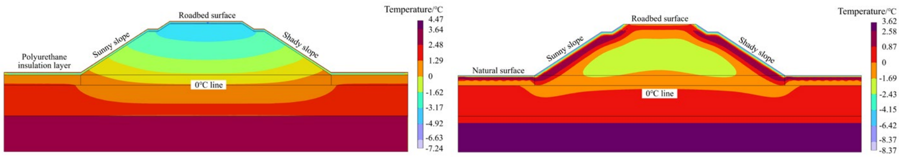

a. Original roadbed b. Processed roadbed

Fig. 3. Cloud map of roadbed temperature field

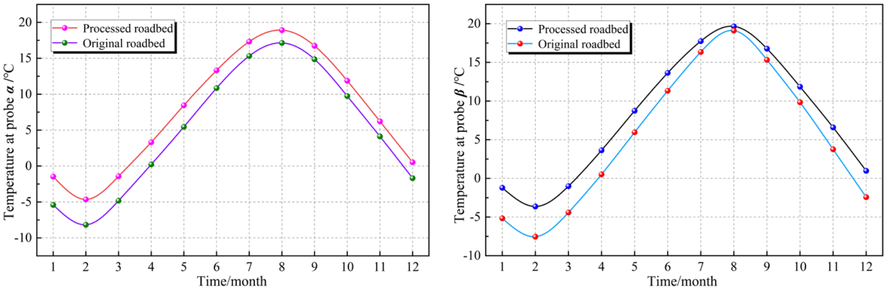

a. Temperature at point α b. Temperature at point β

Fig. 4. Annual temperature variation process of roadbed point probe

5.2 Comparative Analysis of Roadbed Displacement Field

The calculation results of the displacement field of the original roadbed and the processed roadbed are shown in Figures 5a and 5b. The frost heave and thaw settlement of the roadbed are the result of the coupling effect of moisture, temperature, and soil stress. The displacement at the sunny-shady slopes caused by solar radiation on the original roadbed is greater than that on the roadbed surface, and the displacement increases closer to the foot of the slope. The center of the roadbed surface experiences subsidence due to thaw settlement, and the overall displacement of the roadbed is greater than 10 mm. The maximum frost heave of the original roadbed is about 33 mm. After the treatment of covering the outer surface of the treated roadbed with polyurethane insulation board, the overall displacement of the roadbed is less than 5 mm, and it is uniform frost heave. There is no melting sinking or sunny-shady slopes phenomenon on the surface of the roadbed, and the displacement of the silty clay frost heave layer is relatively small.

Extracting the displacement change data of the original roadbed and the treated roadbed α, as shown in Figure 6, the annual variation amplitude of the overall displacement of the treated roadbed is smaller. The anti frost heave control measures have reduced the vertical displacement of the original roadbed, reducing the maximum frost heave displacement of the roadbed from 30 mm to below 7 mm, a decrease of 76 %, and the maximum settlement displacement from 4 mm to below 1.5 mm, a decrease of 62 %. And it eliminates the uneven frost heave effect under the influence of solar radiation, improving the safety of railway subgrade structures.

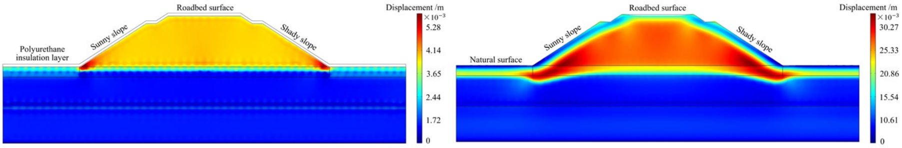

a. Original roadbed b. Processed roadbed

Fig. 5. Roadbed displacement field cloud map

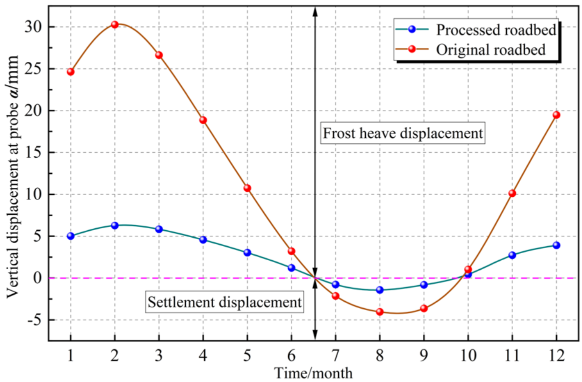

Fig. 6. Vertical displacement variation process at the point probe α in the roadbed domain

6 Conclusion

1. Establishing a transient calculation model for roadbed water heat force coupling frost heave, and verifying the rationality of the numerical model with on-site measured data.The results show that the uneven frost heave degree of the subgrade is exacerbated by the shadow-sun effect caused by solar radiation, leading to an increased variation in the subgrade temperature. The accumulation of water in the silty clay layer at the lower part of the subgrade is identified as the primary cause of frost heave.
2. Compared to the original subgrade, the subgrade treated with anti-frost heave measures exhibits a more uniform overall temperature distribution, reducing the impact of the shadow-sun effect. This alleviates the phenomenon of uneven frost heave and the variation in subgrade displacement, and reduces the vertical frost heave of the soil.
3. The calculation results indicate that the insulation, waterproofing, and anti-frost heave measures reduced the railway subgrade frost heave displacement by 76 %, which can effectively address the frost heave settlement problem in existing railway

subgrades in frozen soil regions. This improves the safety and stability of the railway subgrade structure and has promising engineering application prospects.

References

1. Zang H.W, Wang X.Y, Zhao X, et al. (2020) In situ experiment investigations of hydrothermal process of highway in deep seasonal frozen soil regions of Inner Mongolia, China[J]. Journal of Central South University, 27(7): 2082 - 2093.
2. Cai X.P, Zhang Q, Zhang Y.R, et al. (2021) Deformation law and control limit of CRTS III slab track under subgrade frost heave[J]. Applied Sciences, 11(8): 3520.
3. Wang Q.Z, Tal B.W, Liu Z.Y, et al. (2018) Study on the sunny-shady slope effect on the subgrade of a high-speed railway in a seasonal frozen region[J]. Sciences in Cold and Arid Regions, 7(5): 513 - 519.
4. AGGESTAM E, NIELSEN J C O. (2019) Multi-objective optimisation of transition zones between slab track and ballasted track using a genetic algorithm[J]. Journal of Sound and Vibration, 446: 91 - 112.
5. PIOTROVICH A A, ZHDANOVA S M. (2015) To the issue of stabilization of permafrost soil subgrade[J]. Sciences in Cold and Arid Regions, 7(4): 329 - 334.
6. Zhao G.T, Liu X.B, Gao L, et al. (2016) Characteristic analysis of track irregularity in subgrade frost heave area of Harbin-Dalian high-speed railway[J]. Journal of the China Railway Society, 38(7): 105 - 109.
7. NISHIMURA S, GENS A, OLIVELLA S, et al. (2009) THM coupled finite element analysis of frozen soil: Formulation and application [J]. Géotechnique, 59(3): 159 - 171.
8. Yang G.S, Liu Y.M, Gao Y.F, et al. (2021) Coupled thermo-hydro-mechanical process in buffer material and self-healing effects with joints [J]. Journal of Central South University, 28(9): 2905 - 2918.
9. Zhang Y.Z, Sun B.C, Wen A, et al. (2019) Transverse thermal difference of high-speed railway roadbed in seasonally frozen regions [J]. Proceedings of the Institution of Civil Engineers-Ground Improvement, 172(4): 264 - 273.
10. Lu X.F, Zhang F, Tang K.W, et al. (2021) Field monitoring of differential frost heave in widened highway subgrade[J]. Sciences in Cold and Arid Regions, 13(5): 408 - 418.
11. Ren J.J, Zhang K.Y, Zheng J.L, et al. (2022) Railway subgrade thermal-hydro-mechanical behavior and track irregularity under the sunny-shady slopes effect in seasonal frozen regions[J]. Journal of Central South University, 29(11): 3793 - 3810.